CO hydrogenation towards higher alcohols catalysed on SiO_2-grafted and zeolite-entrapped Ru, Co and RuCo bimetallic clusters: their EXAFS and FTIR characterization and catalytic performances

G.-C. Shen [a], A.-M. Liu [a,b], Takafumi Shido [a] and Masaru Ichikawa [a]

[a] *Catalysis Research Center, Hokkaido University, Sapporo 060, Japan*
[b] *Dalian Institute of Chemical Physics, Chinese Academy of Sciences, Dalian, PR China*

Some Ru and Co carbonyl clusters in zeolite pores such as $Ru_3(CO)_{12}$/NaY, $[HRu_6(CO)_{18}]^-$/NaY, $[Ru_6(CO)_{18}]^{2-}$/NaX, $Co_4(CO)_{12}$/NaY and $Co_6(CO)_{16}$/NaY were prepared by the ship-in-bottle technique, and characterized by FTIR and EXAFS. The RuCo bimetallic carbonyl cluster was prepared by reductive carbonylation of the oxidized RuCo/NaY, which provides the proposed assignment to $[HRuCo_3(CO)_{12}]$/NaY. The tailored Ru, RuCo and Co catalysts were prepared by H_2 reduction from the precursors, e.g. Ru, RuCo bimetallic and Co carbonyl clusters impregnated on SiO_2 and entrapped in NaY and NaX zeolites. The RuCo bimetallic carbonyl cluster-derived catalysts showed substantially higher activities and selectivities for oxygenates such as C_1–C_5 alcohols in CO hydrogenation ($CO/H_2 = 0.33$–1.0, 5 bar, 519–543 K). By contrast, hydrocarbons such as methane were preferentially obtained on the catalysts prepared from Ru_6, Ru_3 and Co_4 carbonyl clusters and provided lower CO conversion and poor selectivities for oxygenates. The RuCo bimetals are proposed to be associated with the selective formation of higher alcohols in CO hydrogenation.

Keywords: CO hydrogenation; EXAFS characterization; FTIR characterization; Ru, RuCo and Co carbonyl clusters in NaY and NaX zeolites

1. Introduction

It has been previously reported that some metal additives, such as Fe, Zn, and Mo, promote the production of alcohols in CO hydrogenation on modified Rh, Pt, Ir and Pd catalysts [1,2].

As a localized model for Rh, Ir and Pd bimetal catalysts have been prepared from SiO_2-grafted $FeRh_4$, Fe_2Rh_4, $FeIr_4$ and Fe_6Pd_6 carbonyl clusters, and it has been demonstrated that the Fe promoted Rh, Ir and Pd cluster-derived catalysts provided substantially high activity and selectivity for methanol and ethanol formation in CO hydrogenation [3,4]. EXAFS [5], and ^{57}Fe Mössbauer [6] studies of the cluster-derived Rh–Fe/SiO_2 catalysts suggested that this promotion was associated with the two-site CO activation to enhance the CO insertion on Rh–Fe^{3+}

sites localized on the $RhFe/SiO_2$ interface. Furthermore, it has been reported recently [7,8] that the SiO_2-supported catalysts prepared from RuCo bimetallic carbonyl clusters exhibited higher selectivities towards C_1–C_5 alcohols in CO hydrogenation than those on the uncombined Ru or Co catalysts. Accordingly, in this work, to obtain more insight into the local structures of RuCo bimetal sites to promote the higher alcohol formation in CO hydrogenation, attempts have been made to prepare some Ru, RuCo and Co carbonyl cluster compounds impregnated on SiO_2 and occluded inside NaY and NaX zeolites by the "ship-in-bottle" technique [3,9,10]. The intrazeolite mono- and bimetal carbonyl clusters are characterized by FTIR and EXAFS spectroscopies. The catalysts derived from RuCo bimetal carbonyl clusters grafted on SiO_2 and in NaY zeolites are studied in conjunction with the promotion of activities and selectivities for C_1–C_5 alcohol formation in the $CO + H_2$ reaction.

2. Experimental

2.1. PREPARATION OF CATALYSTS

Syntheses of clusters in zeolites and their impregnation onto SiO_2 were carried out using standard Schlenk and needle stock techniques, similarly as reported previously [6–8]. A series of tailored bimetallic catalysts have been prepared using silica-grafted bimetal carbonyl cluster compounds such as $Ru_6C(CO)_{17}$, $[NEt_4][HRu_3(CO)_{11}]$, $Ru_3Co_3C(CO)_{14}$, $[Et_4N]_2[Fe_3Ru_3C(CO)_{17}]$, $HRuCo_3(CO)_{12}$, $[Et_4N]_2[Mo_2Ru_3(CO)_{16}]$, $[Et_4N]_2[MnRu_3C(CO)_{14}]$ and $[PPN]_2[Cr_2Ru_3C(CO)_{16}]$ as the metal precursors, which were grafted on amorphous silica (surface area 280 $cm^2\ g^{-1}$, Davison No. 57).

2.2. SHIP-IN-BOTTLE SYNTHESIS OF Co, Ru AND RuCo CARBONYL CLUSTERS IN NaY AND NaX ZEOLITES

The samples containing 3.2 wt% Ru were prepared by cation-exchange of NaY (LZY-52 from TOSO Chem. Co. Si/Al = 5.6) and NaX (Union Showa K.K. 13X, Si/Al = 2.3) with $[Ru(NH_3)_6]Cl_3$ aqueous solution at 300 K for 2 days. After filtering and washing in deionized water, the samples were dried at 393 K, and were exposed to a $CO + H_2$ mixture (200/200 Torr) in a closed circulating reactor by temperature-programmed heating from 300 to 354–413 K, resulting in $[HRu_6(CO)_{18}]^-$/NaY [I] characteristic of IR carbonyl bands at 2126(w), 2062(vs), 2044(s), and 1975(s) cm^{-1}; and $[Ru_6(CO)_{18}]^{2-}$/NaX [II] (2000(w), 1970(vs), 1743(m) cm^{-1}; 235, 285 nm (UV–vis)), respectively. Similarly, the reductive carbonylation of $Co_2(CO)_8$/NaY (10 wt% Co) was carried out in a Pyrex-glass reactor under 300 Torr of CO and 100 Torr of H_2 at 313 K for 36 h to give $Co_6(CO)_{16}$/NaY [III] (ν_{CO} = 2080(s) and 1716(s) cm^{-1}). Synthesis of the bimetallic RuCo car-

bonyl clusters was tried by the reductive carbonylation of oxidized [I] combined with $Co_2(CO)_8$ by flowing a CO + H_2 mixed gas at 313–393 K. The resulting sample shows the IR bands at ν_{CO} = 2080(s), 2056(m), 1972(sh) and 1813(s) cm^{-1}, and is designated as [IV]. $Co_4(CO)_{12}$/NaY [V] characteristic of the carbonyl bands at 2126(w), 2078(s) and 1817(m) cm^{-1} was prepared by the immersion of a NaY pellet into $Co_2(CO)_8$ under a wet CO atmosphere at 323 K, according to the literature method [11]. $Ru_3(CO)_{12}$ in NaY (4 wt% Ru) designated as $Ru_3(CO)_{12}$ was prepared by vapor deposition at 323–363 K; it showed the characteristic IR carbonyl bands (ν_{CO} = 2124(w), 2068(s), 2028(s) cm^{-1}; diffused reflectance UV–vis, 234, 392 nm).

2.3. CATALYST PREPARATION

The cluster-impregnated samples, such as SiO_2-grafted and zeolite-encaged Ru, Co and RuCo carbonyl clusters, were, after removal of the solvents, subjected to mild oxidation with O_2 at 423 K for 2 h in a glass-tube, followed by reduction in H_2 flow (1 bar, 40 ml/min) at the programmed temperature from 293 to 573 K for 2 h and 573 K for 2 h. The sample was transferred to a microreactor and reduced again in H_2 flow at 573 K for 1 h prior to introducing syngas for CO hydrogenation.

2.4. CO HYDROGENATION

The CO hydrogenation reaction was carried out at 422–523 K with a continuous-flow stainless-steel microreactor (18 mm diameter × 300 mm long), where 0.50 g of the Ru_4/NaY (Ru_6/NaX) catalyst (Ru loading 3.2 wt%) or Co_4/NaY (Co 10 wt%) was charged. A gas mixture of CO and H_2 (CO/H_2 = 0.33 v/v, 5×10^5 Pa) was introduced into the reactor at a flow rate of 40 ml/min and a space velocity of 4800 h^{-1}. Oxygenate products, including alcohols and aldehydes, were collected in a 50 ml water trap by bubbling the effluent gas through it. The products were analyzed by the thermal conductivity detector (TCD) and flame ionization detector (FID) of a gas chromatograph (Shimadzu GC-8A) using active carbon, alumina-N,N-dimethylformamide (DMF 38%, 60–80 mesh), and Squalane columns for CO, CO_2, hydrocarbons, and oxygenates, respectively.

2.5. INFRARED AND UV–VIS EXPERIMENTS

The catalysts (Ru and Co loading 3–10 wt%) were pressed into self-supporting disks (15 mm i.d., 12–20 mg cm^{-2}) and were placed into an infrared cell equipped with CaF_2 windows. Infrared and UV–vis spectra were measured under various conditions using a Fourier transform spectrometer (Shimadzu double beam FTIR-4100) with a resolution of 2 cm^{-1} and Hitachi-330 spectrophotometer. For the iso-

tope-labelling experiments ^{13}CO (90% enriched) and D_2 (99.9%) were purchased from MSD Isotope Co.

2.6. EXAFS SPECTROSCOPY

The catalysts (Ru and Co loading 3–10 wt%) were pressed into self-supporting disks (15 mm, i.d., and 30 mg) and pressed into the stainless-steel chamber with an ultra high vacuum (10^{-6} Pa). EXAFS measurements were carried out at SOR beam line 10B of the Photon Factory in the National Laboratory for High Energy Physics (KEK-PF) using synchrotron radiation with an electron energy of 25 GeV at current of 100–250 mA. The EXAFS (extended X-ray absorption fine structure) spectra were measured at the Ru K edge (22121 eV) and Co K (7710 eV) using a Si(111) double crystal monochromator. The analyses of EXAFS data were derived by the Fourier transform curve-fitting method using the computer program PROGRAM 2, as described elsewhere [6,9,10].

3. Results and discussion

3.1. FTIR AND EXAFS CHARACTERIZATION OF Ru, Co AND RuCo CARBONYL CLUSTERS IN NaY AND NaX ZEOLITES

A typical set of infrared spectra resulting from the reductive carbonylation of $[Ru^{3+}(NH_3)_6]/NaX$ with $CO + H_2$ mixture at 300–393 K are shown in fig. 1. Table 1 summarizes the results of this experiment and the other Ru carbonyl species as references. The resulting samples after exposure to $CO + H_2$ at 300–353 K (fig. 1b) gave the bands at 2072, 2000 and 1939 cm^{-1}, which are assigned to $[Ru^{II}(NH_3)_5CO]$. Simultaneously, the band at 1356 cm^{-1} due to N–H stretching of NH_3 was greatly diminished, and at the expense of this band a new band appeared at 1469 cm^{-1} attributed to ν_4, δ(N–H) of NH_4^+ ions, implying that the reaction of $NH_3 + H_2O$ proceeds to give NH_4^+ ions and basic OH in NaX zeolite pores. When the temperature was raised to 393 K, the spectrum yields two sets of peaks at (2088, 2014) and (2048, 1952) cm^{-1} (fig. 1c), possibly attributable to $Ru^I(CO)_2$ and $Ru^I(CO)_3$, respectively [12]. After a prolonged reaction at 393 K, the intermediate subcarbonyls were eventually converted to the stable carbonyl cluster characteristic of the carbonyl bands (fig. 1d) at 2000(s), 1970(m), 1743(m) and 1702(w) cm^{-1} (diffuse reflectance UV–vis; $\lambda_{max} = 235$, 285 nm). This spectrum closely resembles that of $[PPN]_2[Ru_6(CO)_{18}]$ in dichloromethane ($\nu_{CO} = 2000$(s), 1986(s), 1930(sh) and 1754(m) cm^{-1}) (UV–vis; 235, 287 nm) [13], except for the blue shift of linear CO and red shift of bridging CO frequency for the sample. The CO frequency shifts of intrazeolite Ru_6 carbonyl clusters is explained by the interaction between O-ended carbonyl in the Ru carbonyl clusters and the acid sites in NaX zeolites, similarly for $[Rh_6(CO)_{16}]/NaY$ [9] and $[Pt_{12}(CO)_{24}]^{2-}/NaY$ [10].

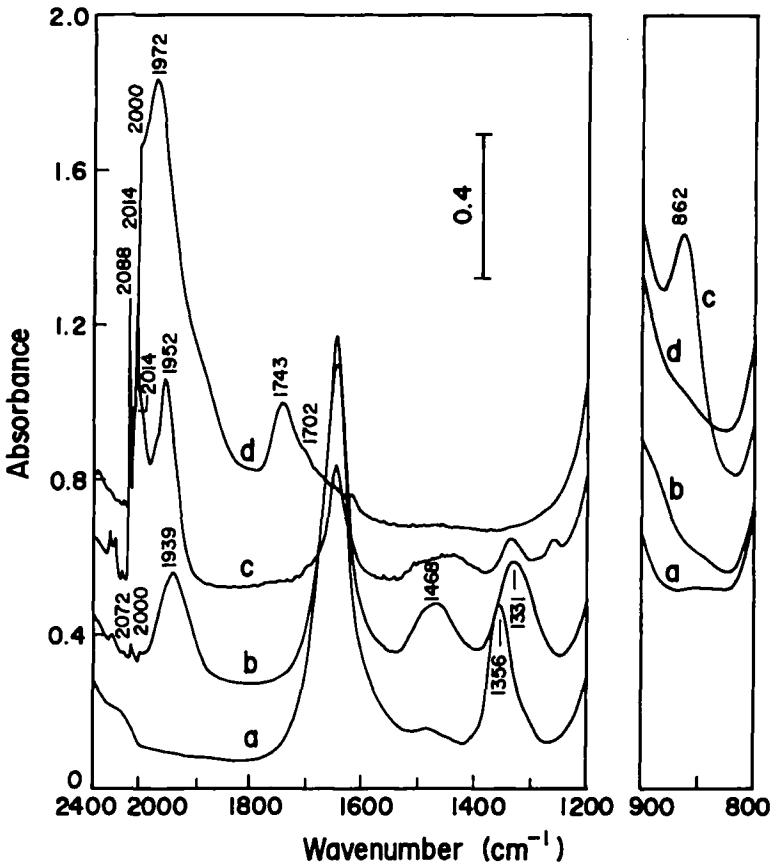

Fig. 1. In situ FTIR spectral changes in the carbonyl stretching region for the reaction of $Ru^{III}(NH_3)_6$/NaX with CO + H_2 (200 Torr/200 Torr) at (a) 298 K, (b) 353 K, (c) 393 K for 0.5 h, and (d) 393 K for 46 h.

The EXAFS measurements were carried out in transmission mode at 13L-10B of the Photon Factory in the National Laboratory for High Energy Physics. Fig. 2 presents the raw EXAFS function and its Fourier transform for the sample of proposed $[Ru_6(CO)_{18}]^{2-}$/NaX [II]. The raw EXAFS function (fig. 2a) shows oscillations up to a value of k of above 15 $Å^{-1}$, clearly indicating the presence of near-neighbour high-atomic-weight backscatterers, which are inferred to be Ru. The EXAFS spectrum for $k > 11$ $Å^{-1}$ is almost entirely due to the Ru–Ru shell. Table 2 lists the results of the data analysis for the $[Ru_6(CO)_{18}]^{2-}$/NaX sample. The Ru–Ru coordination number of 3.5 suggests the presence of a cluster, with only 4–6 Ru atoms, while the Ru–Ru distance of 2.82 Å is reasonably consistent with that for $[PPN]_2[Ru_6(CO)_{18}]$ in crystal measured by X-ray analysis (2.80–2.89 Å) [14]. Note that besides the $[Ru_6(CO)_{18}]^{2-}$ cluster dianion there are minor contributions of subcarbonyls such as $Ru^I(CO)_x$ ($x = 2, 3$) which are bonded to zeolite support oxygen (less than 15% of total Ru in NaX). A reasonable explanation is provided by the

Table 1
Carbonyl stretching frequencies

System	Carbonyl stretching frequencies (cm^{-1})
$Ru^{I}(CO)_2$/NaX	2080s, 2010s
$Ru^{I}(CO)_3$/NaX	2040s, 1988s
$Ru_3(CO)_{12}$/NaY	2124w, 2068vs, 2028s
$Ru_3(CO)_{12}$ in hexane	2062vs, 2032s, 2011m
$[PPN]_2[Ru_6(CO)_{18}]$ in CH_2Cl_2	2006s, 1986s, 1930m and 1758w (UV–vis; 235, 287 nm)
$[Ru_6(CO)_{18}]^{2-}$/NaX	2014s, 1972s, 1743m, 1702w (diffuse reflectance UV–vis; λ_{max} = 235, 285 nm).
$[HRu_6(CO)_{18}]^{-}$/NaY	2126w, 2062vs, 2044w, and 1975m
$[PPN][HRu_6(CO)_{18}]$ in CH_2Cl_2	2027vs, 1957m
$Ru_6C(CO)_{16}^{2-}$ in CH_2Cl_2	2048w, 2032w, 1977s, 1957m, 1918m, 1980m
$Ru_6C(CO)_{17}$ in CH_2Cl_2	2065s, 2046s, 1995w, 1851w

minor contribution of mononuclear Ru carbonyl, which results in the observed Ru–Ru coordination number less than 4 for the Ru_6 octahedron framework.

By contrast, it is interesting to find that the ion-exchanged $[Ru^{3+}(NH_3)_6]$/NaY in the CO + H_2 reaction at 393–423 K showed the IR carbonyl spectrum (ν_{CO} = 2126(w), 2062(vs), 2044(sh), and 1975(m) cm^{-1}) with no bridging CO, which is different from that of $[Ru_6(CO)_{18}]^{2-}$/NaX. The resulting spectrum rather resembles that of $[PPN][HRu_6(CO)_{18}]$ in solution (2027(vs) and 1957(m) cm^{-1} [15]) except for the CO frequency shifts. The formation of protonated Ru_6 dianion in NaY might be owing to more acidic circumstances in NaY cages, compared with that in NaX. The EXAFS parameters for the proposed sample of $[HRu_6(CO)_{18}]^{-}$/NaY (I) are listed also in table 2, suggesting that the NaY zeolite is encaged with the carbonyl cluster consisting with the Ru_6 octahedron framework similar to $[Ru_6(CO)_{18}]^{2-}$/NaX (II).

The zeolite-occluded $[Co_4(CO)_{12}]$/NaY (V) obtained by vapor-phase immersion of an NaY zeolite pellet into $Co_2(CO)_8$ at 300–323 K is characteristic of the IR carbonyl bands at 2126(w), 2078(s) and 1817(m) cm^{-1}. The bands are shifted significantly from $Co_4(CO)_{12}$ deposited on NaY (2064, 2055, and 1868 cm^{-1}). The sample was readily decarbonylated upon exposure to oxygen at 300–323 K to give the oxidized species designed as $[Co_4O_x]$/NaY. The oxidized sample was successively reduced with H_2 at 523 K for 20 h. The EXAFS measurements were carried out for these samples and the Fourier transform spectra are shown in fig. 3. The EXAFS parameters (CN = 3.2 and r = 2.6 Å) for the H_2-reduced sample derived from $[Co_4(CO)_{12}]$/NaY suggest that the highly dispersed reduced cobalt cluster (less than 6 Å in size) designated as $[Co_4]$/NaY is relatively stabilized to be encaged in the NaY pores.

After immersion of the NaY zeolite pellet into a pentane solution of $Co_2(CO)_8$, the impregnated wafer was, after removal of the solvent, gently heated from 300 to 323 K under a mixture gas of CO (300 Torr) and H_2 (100 Torr). Fig. 4a shows

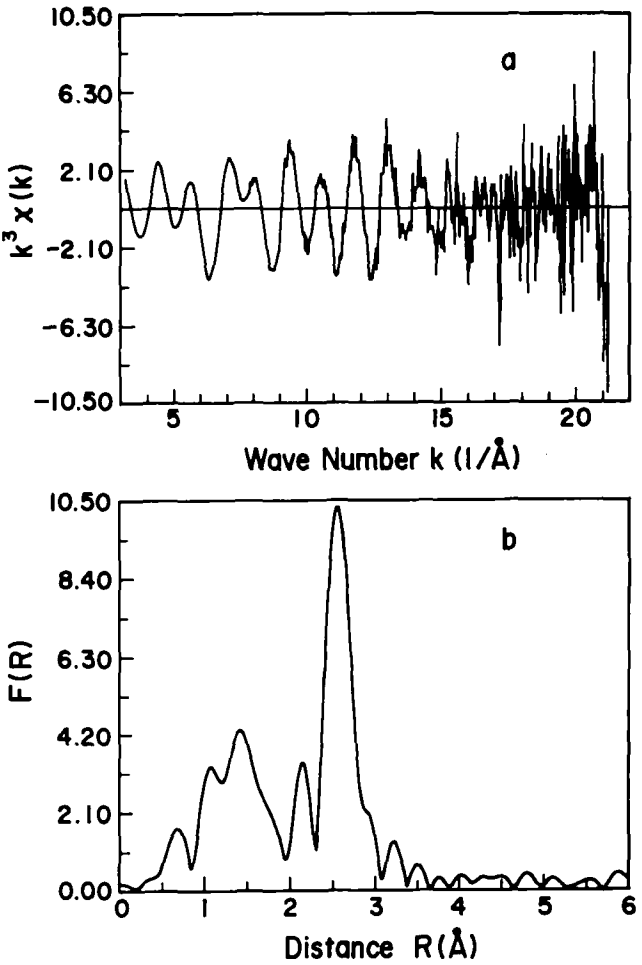

Fig. 2. Ru K-edge EXAFS data for $[Ru_6(CO)_{18}]^{2-}$/NaX (II); (a) k^3-weighted EXAFS oscillation, (b) associated Fourier transform.

the successive in situ FTIR spectra obtained after the reaction for 1–36 h, where two intense IR carbonyl bands at 2080 and 1719 cm^{-1} were developed on time of stream. The spectrum resembles $Co_6(CO)_{16}$ in solution (2061(vs), 2057(sh),

Table 2
Ru K-edge EXAFS results for $[Ru_6(CO)_{18}]^{2-}$ in NaX zeolite [a]

Shell	CN	R (Å)	ΔE_0 (eV)	σ (Å)
Ru–Ru	3.5	2.82	12.85	0.067
Ru–C	3.1	1.86	−6.67	0.060
Ru–O	1.4	2.26	3.66	0.085

[a] CN, R, ΔE_0 (eV), and σ (Å) represent coordination number, interatomic distance, change in energy threshold, and Debye–Waller factor, respectively.

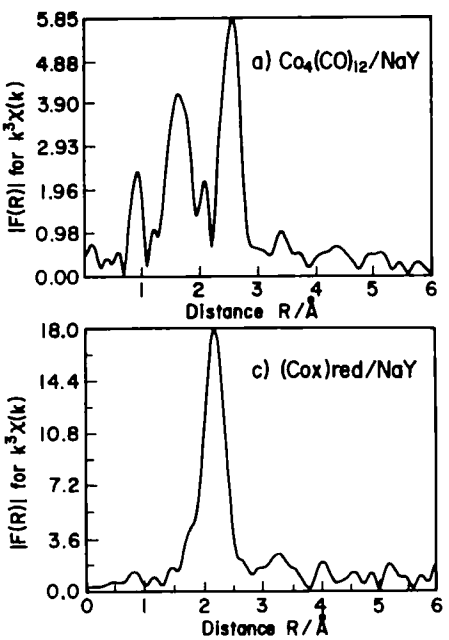

			C.N.	R/Å
a)	$Co_4(CO)_{12}$	Co-Co	2.0	2.54
		Co-C	2.1	2.05
	Co Foil		12	2.48
b)	(Cox)ox/NaY	Co-O	1.8	2.02
c)	(Cox)red/NaY	Co-Co	2.9	2.49

Fig. 3. Fourier transforms of k^3-weighted EXAFS spectra; $k^3\chi(k)$ versus R (Å). (a) $Co_4(CO)_{12}$/NaY, (b) Co_4O_x/NaY (oxidized), and (c) Co_4/NaY (reduced), including the evaluated EXAFS parameters.

1772 cm^{-1}) [16], except for the blue shift of linear CO and the red shift of bridging CO frequency possibly due to the intrazeolite occlusion. Fig. 4b represents a set of in situ IR spectra of ^{13}CO exchange reaction with $[Co_6(CO)_{16}]$/NaY at 300 K, implying that the facile CO exchange occurs to give the NaY-encaged $Co_6(^{13}CO)_{16}$ (ν_{CO} = 2028(vs) and 1673(s) cm^{-1} in fig. 4a).

3.2. FORMATION OF RuCo BIMETALLIC CLUSTERS IN NaY

Fig. 5 shows the IR carbonyl spectra obtained upon immersion of the oxidized $[HRu_6(CO)_{18}]^-$/NaY (3.2 wt% Ru) (I) pellet into a pentane solution of $Co_2(CO)_8$ (Co/Ru = 3 atomic ratio). The resulting spectra were obtained after the subsequent reaction with Co + H_2 at 323–393 K, characteristic of the carbonyl bands at 2080(vs), 2060(s), 1980(m) and 1813(s) cm^{-1}. It is interesting that they resemble those of $HRuCo_3(CO)_{12}$ (ν_{CO} = 2070(vs), 2062(vs), 2030(s) and 1884(s) in acetone) [17], except for the blue frequency shift of linear CO and the red shift of bridging CO for the carbonyl cluster in NaY. By comparison with the IR carbonyl bands of the sample, it is not likely attributable to $[RuCo_3(CO)_{12}]^-$(ν_{CO} = 2024(vs), 1996(vs), 1967(s), 1887(m) and 1813(s) cm^{-1} in CH_2Cl_2) nor to $HCoRu_3(CO)_{13}$ (2013(s), 2061(vs), 2054(vs), 2034(m), 2024(m), 2017(m) cm^{-1} in hexane solution) [18]. The resulting intrazeolite RuCo bimetal carbonyl cluster is

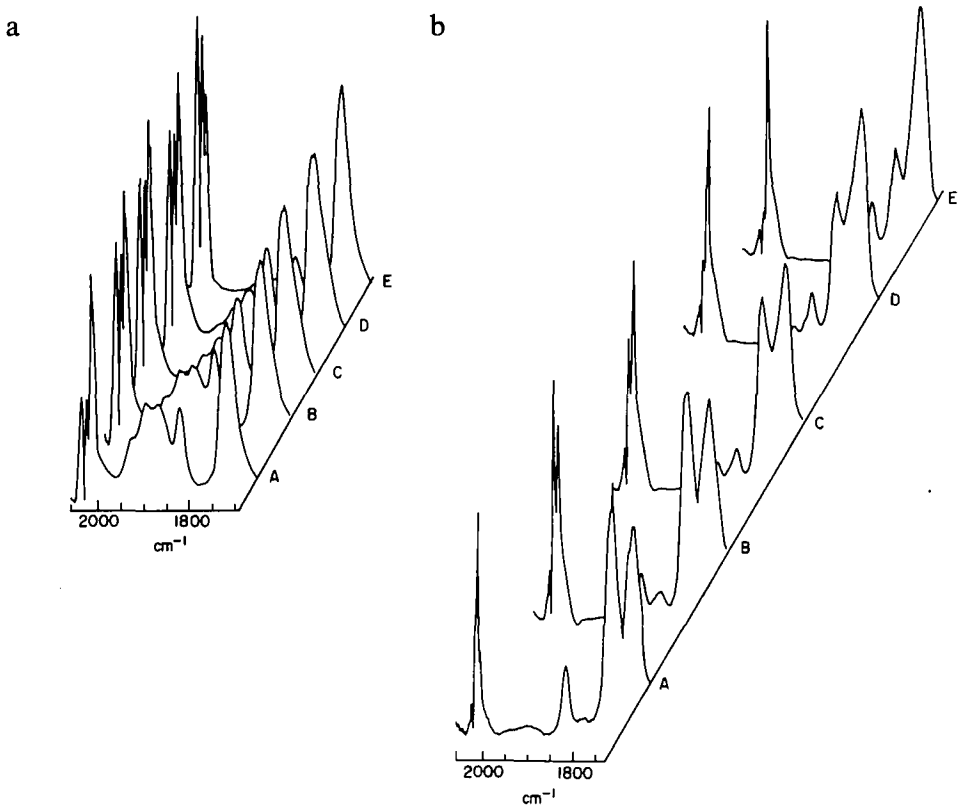

Fig. 4. (a) In situ FTIR spectral changes in the carbonyl region for formation of $Co_6(CO)_{16}$/NaY in the reaction of impregnated $Co_2(CO)_8$/NaY with CO + H_2 (300 Torr CO/100 Torr H_2) at 313 K after (A) 1 h, (B) 5 h, (c) 12 h, (D) 24 h, and (E) 36 h. (b) In situ FTIR spectral changes in the carbonyl region for ^{13}CO exchange reaction with $Co_6(CO)_{16}$/NaY at 300 K (100 Torr of ^{13}CO) after (A) 1 h, (B) 4 h, (C) 6 h, (D) 8 h, and (E) 10 h.

designated as $[HRuCo_3(CO)_{12}]$/NaY (IV). The intrazeolite formation of $HRuCo_3(CO)_{12}$ in NaY cages may be analogous with the homogeneous preparation which is accomplished by allowing $Na[Co(CO)_4]$ to react with $RuCl_3$ in refluxing methanol solution followed by protonation with H_3PO_4 [17],

$$3Na[Co(CO)_4] + RuCl_3 \rightarrow Na[RuCo_3(CO)_{12}] + 3NaCl$$
$$[RuCo_3(CO)_{12}]^- + H_3PO_4 \rightarrow HRuCo_3(CO)_{12}\,.$$

3.3. SiO_2-GRAFTED RuM BIMETALLIC CLUSTER-DERIVED CATALYSTS IN CO HYDROGENATION

The catalytic activity of SiO_2-grafted RuM carbonyl cluster-derived catalysts reached the steady state of CO conversion and product selectivities orienting toward alcohols after 10–15 h on stream in CO hydrogenation, and remained basi-

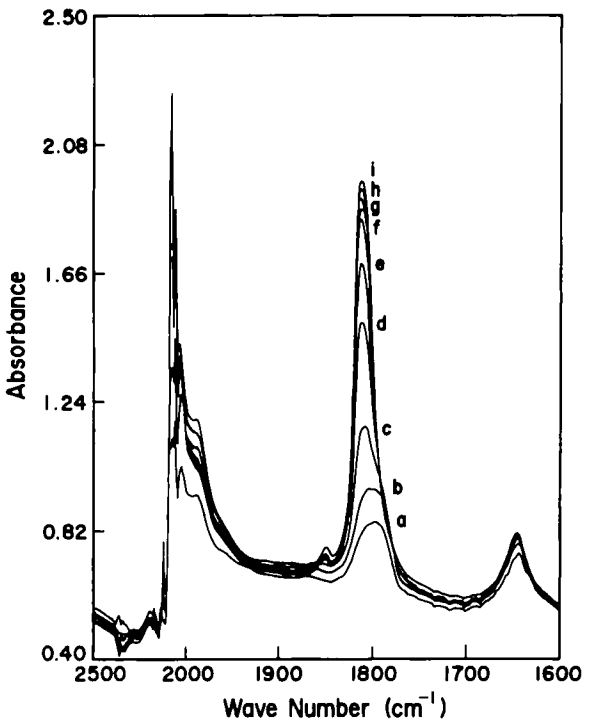

Fig. 5. In situ FTIR spectral changes in the carbonyl region for formation of $HRuCo_3(CO)_{12}$/NaY in the reaction of the oxidized $[HRu_6(CO)_{18}]^-$/NaY (I) combined with the immersion of $Co_2(CO)_8$ under the atmosphere of CO + H_2 (300 Torr CO/100 Torr H_2) at 353 K after (a) 0.5 h, (b) 1 h, (c) 4 h, (d) 6 h, (e) 6 h, (f) 8 h, (g) 12 h and (i) 16 h.

cally constant for a subsequent 45–50 h. Catalytic performances for various products, including hydrocarbons and oxygenates in CO hydrogenation at 519 K are presented in table 3, where the selectivities were based on CO. The monometallic catalysts derived from $HRu_3(CO)_{11}$, $Ru_6C(CO)_{17}$ and $Co_4(CO)_{12}$ provided high rates of hydrocarbons (C_1–C_5) with negligible amounts of oxygenates. The SiO_2-grafted catalysts derived from Ru carbido-clusters such as $Ru_6C(CO)_{17}$ gave no particular improvement of alcohol formation in CO hydrogenation, compared with those from Ru carbonyl clusters in contrast to those on MgO-impregnated catalysts [19]. However, it is of interest to find that the catalysts from the SiO_2-grafted RuM (M = Co, Fe, Ni and Cr) bimetallic carbonyl clusters exhibited the following features in CO hydrogenation: (a) the CO conversion and activities for oxygenates toward C_1–C_5 alcohols were enhanced substantially on the catalysts from $Ru_3Co_3C(CO)_{14}$, $RuCo_2(CO)_{11}$ and $HRuCo_3(CO)_{12}$ with higher conversion in the higher alcohol selectivities up to 23–38%. (b) the CO conversion on RuFe and RuMo bimetallic catalysts decreased considerably, but the activity for the oxygenates increased relatively, and, as a result, the selectivities for oxygenates consisting of methanol and ethanol in CO hydrogenation were up to 28 and 26% over

Table 3
Catalytic performances of Ru, Co and RuM (M = Co, Fe, Mo, Ni, Mn, Cr) bimetal carbonyl cluster-derived catalysts in CO hydrogenation [a]

Precursor on SiO_2 (1 wt% Ru)	CO conv. (%)	Rate of formation (mmol (mol Ru)$^{-1}$ min^{-1})								Selectivity [b] of oxygenates (%)
		oxygenates				hydrocarbons				
		MeOH	MeCHO	EtOH	$C_{3+}OH$	C_1	C_2	C_3	C_{4+}	
$[HRu_3(CO)_{11}]^-$	0.32	–	–	–	–	16	2	0.3	0.2	0
$Ru_6C(CO)_{17}$	4.9	–	3	–	–	75	11	14	33	2
$RuCo_2(CO)_{11}$	4.4	5	4	8	1	110	12	13	10	13
$HRuCo_3(CO)_{12}$	9.8	12	3	13	3	237	31	30	30	9
(458 K)	1.3	10	2	5	2	24	3	3	3.5	38
$CO/H_2 = 1.0$	4.8	13	4	14	3	98	15	13	10	36
$Ru_3Co_3C(CO)_{16}$	5.5	5	5	8	0.8	145	17	18	14	11
$[Et_4N]_2[Ru_3Fe_3C(C)_{12}]$	1.1	5	1	6	–	3	5	2	–	28
$[Et_4N]_2[Ru_2Mo_2C(CO)_{16}]$	0.7	6	0.5	3	–	18	4	–	–	26
$[Et_4N]_2[Ru_3Ni_3C(CO)_{13}]$	0.5	2	0.4	0.8	0.1	20	3.4	–	–	16
$[Et_4N]_2[Ru_3MnC(CO)_{14}]$	0.1	1	–	+	–	14	1.2	–	–	20
$[Et_4N]_2[Ru_2Cr_2C(CO)_{16}]$	0.1	1	–	–	–	6	0.4	–	–	12
$RuCl_3 + CoCl_2$	2.2	0.6	0.8	0.5	–	46	6	7	10	2
$Co_4(CO)_{12}$ [c]	0.1	0.4	0.2	–	–	5	0.4	–	–	1

[a] $CO/H_2 = 0.5$ v/v, flow rate: 40 ml/min, total pressure 5×10^5 Pa.
[b] Molar ratio of $\sum_i C_i$ (i = 1–5, oxygenates)/[oxygenates] + [hydrocarbons] × 100(%).
[c] Rate of formation in mmol (mol Co)$^{-1}$ min^{-1}.

those of RuFe and RuMo catalysts, respectively. (c) RuNi and RuCr catalysts prepared from $[Ru_3Ni_3C(CO)_{13}]^{2-}$ and $[Ru_3Cr_2C(CO)_{16}]^{2-}$ led to a deep decrease in activities for both hydrocarbons and oxygenates. The above results indicate that the RuCo and RuFe bimetallic catalysts are among the best catalysts for formation of higher alcohols, especially for the RuCo carbonyl cluster-derived catalysts. However, some other metals such as Ni, Mn and Cr are not effective to promote the production of oxygenates on the modified Ru catalysts.

3.4. CO HYDROGENATION ON THE CATALYSTS DERIVED FROM Ru, Co AND RuCo CLUSTER IN NaY AND NaX

The catalytic properties of the various catalysts derived from the zeolite-entrapped Ru, RuCo and Co carbonyl clusters in 5 bar $Co + H_2$ reaction at 498–548 K were investigated, and the results are presented in table 4. Interestingly, it is found that the oxygenates such as methanol, formaldehyde and ethanol were produced with relatively higher selectivities on the catalysts prepared from Ru carbonyl clusters in NaY zeolite such as $[Ru_3(CO)_{12}]$/NaY and $[HRu_6(CO)_{18}]^-$/NaY, compared with those on SiO_2-impregnated ones, as shown in table 3. The promotion for alcohol formation may be associated with the basic circumstance in the zeolite cages. Furthermore, the activity and selectivity for the products in CO hydrogenation on various catalysts show a large difference depending on the precursors in NaY and NaX zeolites. The Ru_3/NaY catalyst prepared from $[Ru_3(CO)_{12}]$/NaY has activity for hydrocarbons mainly consisting of methane and forms oxygenates (lower alcohols and aldehydes of C_1–C_3). The Ru_6/NaY derived from $[HRu_6(CO)_{18}]^-$/NaY produced preferentially methane and higher hydrocarbons such as C_2–C_4 with poor yield of oxygenates. By contrast, Co_4/NaY prepared from $[Co_4(CO)_{12}]$/NaY (10 wt% Co) exhibits a lower CO conversion, but the selectivity for oxygenates is 81.2% including methanol and C_{2+} alcohols. The Co_6/NaY from $[Co_6(CO)_{16}]$/NaY has an improved activity for CO conversion but the oxygenates selectivity is greatly suppressed. It is interesting to find that on the RuCo bimetal catalyst prepared from the proposed $[HRuCo_3(CO)_{12}]$/NaY (Ru/Co = 3, 8.8 wt% metal loading), the CO conversion and the rates for oxygenates such as C_1–C_5 alcohols are substantially increased, similarly on the $RuCo_3/SiO_2$ prepared from $[HRuCo_3(CO)_{12}]/SiO_2$. The results indicate that the Co promotes effectively the higher alcohol formation in CO hydrogenation catalyzed on Ru catalysts in combination with Co, possibly resulting in localized RuCo ensembles derived from the used bimetallic clusters grafted on SiO_2 and entrapped in zeolite pores, similarly as proposed previously for the RhFe and IrFe cluster-derived catalysts [7,8].

4. Conclusion

The conclusions of this study may be summarized as follows: (1) Some well-defined Ru, Co and RuCo carbonyl clusters were prepared by the ship-in-bottle

Table 4
Catalytic performances of CO hydrogenation on Ru, Co and RuCo catalysts derived from NaY and NaX zeolite-entrapped carbonyl clusters [a]

Precursor in zeolite (1 wt% Ru)	Co conv. (%)	Rate of formation								Selectivity [b] of oxygenates (%)
		oxygenates				hydrocarbons				
		MeOH	MeCHO	EtOH	$C_{3+}OH$	C_1	C_2	C_3	C_{4+}	
$[Ru_3(CO)_{12}]/NaY$	1.2	3.5*	2.4	6.3	0.8	58	4.6	2.7	1.2	12
$[HRu_6(CO)_{18}]^-/NaY$	3.9	1.3*	0.5	3.4	1.2	165	11	4.1	3.8	3
$[Ru_6(CO)_{18}]^{2-}/NaX$	5.2	4*	0.2	2.9	1.8	192	28	2.7	6.1	8
$[HRuCo_3(CO)_{12}]/NaY$	6.7	28	7	23	13	227	29	13	8.7	39
$CO/H_2 = 1.0$	3.2	11	4	17	8	89	18	11	10	56
$[Co_4(CO)_{12}]/NaY$	0.23	1.8	–	1.3	0.6	3	0.7	1.2	–	38
$[Co_6(CO)_{16}]/NaY$	0.81	1.2	0.2	0.8	0.5	16	1.8	0.6	0.4	24
$[HRu_6(CO)_{18}]^-/NaY + [Co_6(CO)_{16}]/NaY$	4.8	1.8	0.3	2.7	0.9	276	36	12	7.2	6

[a] $CO/H_2 = 0.33$ v/v, flow rate: 40 ml/min, total pressure 5×10^5 Pa; * including HCHO.
[b] Molar ratio of $\sum_i C_i$ (i = 1–5, oxygenates)/[oxygenates] + [hydrocarbons] × 100(%).
[c] Rate of formation in mmol (mol Co, Ru)$^{-1}$ min^{-1}.

technique, and characterized by FTIR and EXAFS spectroscopies. (2) The catalysts prepared from the RuCo and RuFe bimetal carbonyl clusters grafted on SiO_2 and RuCo entrapped in NaY zeolite exhibited higher activities and selectivities toward C_1–C_5 alcohols in CO hydrogenation, compared with those on uncombined Ru and Co cluster-derived catalysts. (3) The catalytic promotion for higher alcohol formation is proposed to be associated with the adjacent RuCo bimetal sites derived from the bimetal clusters, similarly as on the RhFe and IrFe bimetal cluster-derived catalysts.

References

[1] M. Ichikawa, CHEMTECH 12 (1982) 674;
M. Ichikawa, T. Fukushima and K. Shikakura, *Proc. 8th Int. Congr. on Catalysis*, Vol II (1984) p. 69;
W.M.H. Sachtler and M. Ichikawa, J. Phys. Chem. 90 (1986) 475.
[2] T. Fukushima, H. Arakawa and M. Ichikawa, J. Phys. Chem. 89 (1986) 4440;
T. Fukushima, K. Araki and M. Ichikawa, J. Chem. Soc. Chem. Commun. (1986) 148.
[3] M. Ichikawa, Adv. Catal. 38 (1992) 283.
[4] M. Ichikawa, Polyhedron 7 (1988) 2351;
A. Fukuoka, M. Ichikawa, J.A. Hrijiac and D.F. Shriver, Inorg. Chem. 26 (1987) 3643.
[5] M. Ichikawa and T. Fukushima, J. Phys. Chem. 89 (1985) 1564.
[6] A. Fukuoka, T. Kimura, N. Kosugi, H. Kuroda, Y. Minai, Y. Sakai, T. Tominaga and M. Ichikawa, J. Catal. 126 (1990) 434.
[7] M. Ichikawa, F.-S. Xiao, C.G. Magpanty, A. Fukuoka, W. Henderson and D.F. Shriver, Stud. Surf. Sci. Catal. 61 (1991) 297.
[8] F.-S. Xiao, A. Fukuoka and M. Ichikawa, J. Catal. 138 (1992) 206.
[9] M. Ichikawa, L.-F. Rao, T. Ito and A. Fukuoka, J. Chem. Soc. Faraday Discussion 87 (1989) 321;
L.F. Rao, A. Fukuoka, N. Kosugi, H. Kuroda and M. Ichikawa, J. Phys. Chem. 94 (1990) 5317.
[10] G.-J. Li, T. Fujimoto, A. Fukuoka and M. Ichikawa, Catal. Lett. 12 (1992) 171.
[11] M.C. Coaraway and B.E. Hanson, Inorg. Chem. 25 (1986) 1445.
[12] J.J. Verdonck, R.A. Shoonheydt and P.A. Jacobs, J. Phys. Chem. 87 (1983) 683.
[13] C.T. Hayward and J.R. Shapley, Inorg. Chem. 21 (1982) 3816.
[14] P.F. Jackson, B.F.G. Johnson, J. Lewis, M. McPartlin and W.J.H. Nelson, J. Chem. Soc. Chem. Commun. (1979) 735.
[15] C.R. Eady, B.F.G. Johnson, J. Lewis, M.C. Malatesta, P. Maclin and M. McPartlin, J. Chem. Soc. Chem. Commun. (1976) 945.
[16] P. Chini, Inorg. Chem. 8 (1969) 1207.
[17] M. Hidai, M. Orisaku, M. Ube, Y. Koyasu, T. Kodama and Y. Uchida, Organometallics 2 (1983) 292.
[18] P.C. Steinhardt, W.L. Gladfelter, A.D. Harley, J.R. Fox and G.L. Geoffroy, Inorg. Chem. 19 (1980) 223.
[19] Y. Izumi, S. Chihara, H. Yamazaki and Y. Iwasawa, Shyokubai (Catalysis) 35 (1993) 70.